Electrochimica Acta 259 (2018) 410–418

Contents lists available at ScienceDirect

Electrochimica Acta

journal homepage: www.elsevier.com/locate/electacta

Monolithic ceramic electrode for electrochemical deactivation of *Microcystis aeruginosa*

Yifan Gao, Jinna Zhang**, Xuefeng Bai, Shijie You*

State Key Laboratory of Urban Water Resource and Environment, School of Environment, Harbin Institute of Technology, Harbin 150090, PR China

ARTICLE INFO

Article history:
Received 9 June 2017
Received in revised form
31 August 2017
Accepted 19 October 2017
Available online 2 November 2017

Keywords:
Monolithic ceramic electrode
Electrochemical deactivation
Microcystis aeruginosa

ABSTRACT

Algae bloom is a major environmental problem that may occur in both freshwater and marine water, and thus it is important to develop effective manners for deactivating algae. In this study, we investigated the monolithic ceramic electrode (MCE) for electrochemical deactivation of *Microcystis aeruginosa*, a typical alga found in aquatic system. The results demonstrated that the MCE contained the mixed Magnéli-phases of Ti_4O_7, Ti_5O_9 and Ti_9O_{17}, which could achieve efficient and stable deactivation of *M. aeruginosa* cells and removal of chlorophyll-*a*. The chlorophyll-*a* removal was shown to be positively correlated with the current density applied, reaching the maximum efficiency of 89.2% at reaction time of 120 min. The 8-day re-cultivation experiments showed the dependence of deactivation performance on total coulombs, and the coulombs in excess of 77.4 C could completely deprived the *M. aeruginosa* cells of propagation and proliferation. As shown from atomic force microscopy (AFM), scanning electron microscopy (SEM) and flow cytometric (FC) measurement, the algal cells underwent an irreversible damage of cell structure, isolation of intracellular components and dissolution of cytoplasm-like substances after being attacked by electrochemically produced oxidative species. The solution pH was observed to increase from 8.0 to 9.8 during 120-min electrolysis, which should be the consequence of leakage of cytoplasm containing a variety of small-molecule substances such as protein-, humus-, and sugar-like matters, indicated by 3D excitation-emission matrix (EEM) fluorescence spectra. This study provides a promising electrode material for effective electrochemical deactivation of algae in potential application of water purification.

1. Introduction

Eutrophication is a major environmental concern, which can be accelerated by human activities associated with increased discharge of nitrogen and phosphorus elements into aquatic systems. The algae bloom can lead to grand challenges for drinking water sources, fisheries, recreational water bodies, and ballast water contamination [1]. For example, the algae prevent water body from reoxygenation and light penetration, and the algae in water treatment processes may lead to clogging or fouling of filters, membrane and devices, blooms of algal mats as well as disruption of floc settlement [2]. In addition, to avoid aquatic species invasion, the shipping ballast water has to be free of living algae before it can be discharged into new regions [3]. Some microalga like *Microcytis aeruginosa* (*M. aeruginosa*) can produce microcystins and cyanopeptolins that are highly toxic to aquatic ecosystem and human health [4,5]. Chlorine has long been widely used as an effective disinfectant for deactivation of algae. However, recent concerns on chlorine rise due to its activity to react with organic matters to form carcinogenic disinfection by-products (DBPs) like trichloromethanes and chloroactic acids [6,7]. A number of alternatives such as coagulation, flocculation, dissolved air flotation, filtration, and advanced oxidation process have been developed [8–10], but these approaches may have the problems of low efficiency, instability, and extensive energy consumption.

Electron offers an efficient, versatile, easy-to-operate and clean agent. Driven by the electrons, electrochemical advanced oxidation process can yield numerous kinds of oxidizing species like H_2O_2, $^{\bullet}OH$ or $^{\bullet}O_2^-$ radicals, sulfate radicals, and active chlorine [11,12]. These intermediate components are highly active for oxidizing

* Corresponding author. P. O. Box 2603#, No. 73, Huanghe Road, Nangang District, Harbin, 150090, China.
** Corresponding author. P. O. Box 2603#, No. 73, Huanghe Road, Nangang District, Harbin, 150090, China.
E-mail addresses: zzjjnn_4@163.com (J. Zhang), sjyou@hit.edu.cn (S. You).

https://doi.org/10.1016/j.electacta.2017.10.127
0013-4686/

organic pollutants and sterilizing bacteria or virus for disinfection purpose [13]. Recently, an increasing attention has been paid to deactivation of algae in water using electrochemical system with different types of anode materials. For example, Liang et al. [14] and Xu et al. [15] used Ti–RuO_2 anode for oxidation of *M. aeruginosa* via the generation of active oxidants during electrolysis, and they found the substantial dependence of inhibition on the anode materials, current density, and reaction time and mass transfer. Marcia et al. [16] achieved efficient electrochemical treatment of water containing *M. aeruginosa* in a fixed bed reactor with 3D conductive diamond serving as anodes under continuous operation. The removal of *M. aeruginosa* in water was accomplished by the mixture of electrogenerated oxidants, and the presence of algae could inhibit the production of toxic by-products. The boron-doped diamond (BDD) anode could also be efficient for deactivation of *Chlorella vulgaris* by continuous formation of active chlorine and other chloride oxidation products [17]. Recently, Long et al. [18] reported a significant enhanced removal of *M. aeruginosa* in electrochemical system with BDD anode by simple addition of 0.2 mmol L^{-1} Fe^{2+} at pH-neutral conditions, and they obtained over 99.9% removal of *M. aeruginosa* in 60 min. However, there exists a dilemma for the selection of electrode material in terms of electrical conductivity, electrochemical activity, chemical stability, economic reliability and environmental availability. The BDD has been considered as the most promising candidate [19], but large surface area is necessary to match the capability of scale-up wastewater treatment, which adds the capital cost substantially (*e. g.* \$900 cm^{-2} for BDD).

Titanium suboxides have a crystal structure of oxygen deficiency for every *n*th layer, resulting in the shear planes where 2D chains of octahedra become face sharing to accommodate the deficiency in oxygen [20]. This unique structure leads to a combination of outstanding electrical conductivity approaching to that of metals at room temperature and great corrosion resistance close to that of ceramic materials [21,22]. For example, the most common component of Ti_4O_7 ($n = 4$, under trade name Ebonex®, Atraverda Ltd, U.K.) exhibits a great conductivity of ~1050 S cm^{-1}, which is even higher than that of graphitic carbon (~727 S cm^{-1}) [22]. These properties make Ti_4O_7 suitable for many electrochemical applications, such as cathodic oxygen reduction [23], water splitting [24], as well as pollutant removal [25–29].

The Magnéli-phase titanium suboxides have been shown effective for electro-oxidation of many types of pollutants [30–33]. In our previous study, we developed macroporous monolithic Magnéli-phase titanium suboxides, an electrode material having good conductivity, excellent stability, and high oxygen evolution potential [26]. In particular, the macroporous structure is preferred because it can provide larger electrochemically active surface area. Besides, the protons produced from water oxidation can maintain a much lower local pH in the porous apertures than in bulk solution, which is favorable for increasing the activity of •OH radicals and formation of active chlorine. With the unique structure and properties, the macroporous monolithic titanium suboxides could be used as anode material for not only efficient treating industrial dyeing and finishing wastewater, but also enriching electrochemically active microorganisms in bioelectrochemical systems [34]. The titanium suboxides are able to electrochemically produce loosely adsorbed •OH radicals in the potential region of water discharge, which will be highly desirable for destructing the cell structure and algae deactivation.

In this study, the macroporous monolithic titanium suboxides (*i. e.* monolithic ceramic electrode; MCE) are investigated for electrochemically oxidative deactivation of target *M. aeruginosa*, a most frequently found alga in aquatic environment. First, we characterized the morphology, crystalline structure, and corresponding electrochemical properties of MCE. Second, the material was examined for electrochemical removal of algal cells, chlorophyll-*a*, and the stability. Third, the re-cultivation of algae was tested to evaluate the effectiveness of electrochemical deactivation. Last, the mechanisms for destruction of algae cell were discussed.

2. Materials and methods

2.1. Preparation of monolithic ceramic electrode

The Magnéli-phase MCE, produced from high-temperature reduction of rutile TiO_2 by H_2 was supplied by Ti-Dynamics Co. Ltd. (China). In brief, rutile TiO_2 powders were mixed with water and isopropanol (1:1, v/v) to decrease the capillary force of powders, followed by drying and addition of a 5% (w/w) polyethylene oxide binder. The mixture was compressed at 20 MPa to form a plate shape. The plate blocks were sintered in air at a temperature of 1050 °C for 24 h, and then transferred into a furnace for reduction at H_2 atmosphere at 1050 °C for 4 h in the presence of carbon as porosity-producing agent. The white TiO_2 powers were gradually changed to dark blue suboxides as the oxygen vacancies were generated. The suboxides mixed with a certain amount of binders were hot-pressed into a monolithic ceramic electrode bulk.

2.2. Microalgae and culture

The algae *M. aeruginosa* used in this study were purchased from Biological Resource Center, Institute of Microbiology, Chinese Academy of Sciences (IMCAS-BRC) and the medium culture was BG-11 [14]. The culture was inoculated with 15–20% pure *M. aeruginosa* in sterilized flasks and was cultivated under illumination for 14 days until the cyanobacteria were within logarithm growth phase. The light was continuously supplied by incandescent lamp upon automated 14 h/10 h light/dark cycle at room temperature (25 ± 1 °C). The algae in late exponential growth stage were selected as the target for electrolysis experiments.

2.3. Electrolysis experiments

The electrolysis experiments were conducted in a 125 mL cubic Plexiglas reactor with the dimensions of 5 cm × 5 cm × 5 cm. The apparatus was equipped with MCE anode (effective area of 17.2 cm^{-2}) and a stain steel (SS) cathode, placed in an opposite position with electrodes distance of 5 cm. The culture media were used as the electrolyte to perform batch-mode deactivation experiments by using DC power supply (current density of 1–10 mA cm^{-2}) at reaction time of 0–120 min. The silicone gaskets were used to seal the reactor to avoid water leakage and the agitation was implemented to enhance mass transfer. The reactor was designed to minimize the influence of water reduction during sample collection. All the experiments were carried out at room temperature (25 ± 1 °C) and 1.0 atm pressure.

2.4. Analyses and calculations

The crystalline structure of as-prepared MCE material was identified by using X-ray diffraction (XRD) based on X-ray diffractometer (Bruke D8 Adv., Germany) using CuKα radiation (λ = 0.15406 nm) at a power of 40 keV × 30 mA. The morphology of MCE and algal cells were observed by using field emission scanning electron microscope (Guanta 200F, FEI, U.S.). The high-resolution transition electron microscopy (HRTEM) was performed on F-30ST (Tecnai, FEI). The electrochemical properties of MCE were performed using PARSTAT (CHI750D, Chenhua Co. Ltd.) electrochemical system at room temperature (25 °C). Cyclic

voltammograms (CV) tests were conducted at a scan rate of 50 mV s^{-1} in BG-11 medium with algal cells (density of 1.14–1.23 × 10^{10} cells L^{-1}). The algal cells density was counted using a compound microscope (Olympus) at ×40 magnification with a Thoma counting chamber after preservation in Lugol's iodine. The algal cell counts were carried out according to the method previously reported [35]. The optical algal densities were tested spectrophotometrically at wavelength of 680 nm using the U-3100 UV spectrophotometer (Hitachi Co., Japan).

The chlorophyll-contained samples were filtered and adsorbed on GF/C papers, and then were extracted using 90% acetone. The optical densities (OD) values of the extracts at 750 nm, 663 nm, 645 nm, and 630 nm were examined with 1 cm matched cells. The chlorophyll-*a* concentrations were calculated according to the standard method as

$$\text{Chlorophyll} - a(\text{mg/L}) = [11.64(A_1 - A_4) - 2.16(A_2 - A_4) + 0.1(A_3 - A_4)]v/v_g \quad (1)$$

where A_1-A_4 represents the absorbance at wavelength of 663, 645, 630, and 750 nm, respectively. ν is the volume of extract (5 mL), and ν_g the volume of filtered sample.

The pH values were measured using an Orion 720 pH meter. The flow cytometric (FCM) measurements were performed to evaluate the cell damage during electrolysis. An Accuri C6 flow cytometer (BD Biosciences, Franklin Lakers, NJ, U.S.) equipped with 15 mW argon laser emitting at a fixed wavelength of 488 nm was used for fluorescence measurements. The atomic force microscopy (AFM, Bioscope, Veeco, U.S.) was applied for observing the morphology of algal cells before and after electrolysis. To analyze the composition variation of algal solution, the 3D excitation-emission matrix (EEM) fluorescence spectrum was conducted to characterize the algogenic organic matter produced by *M. aeruginosa* using a fluorescence spectrophotometer (F7000, Hitachi, Japan). To remove the interferences of original existed extracellular organic matter (EOM), the initial harvested algal solution was centrifuged at 4000 rpm for 15 min. The cells at the bottom of the centrifuge tube were collected and re-suspended in the media to be treated by electro-oxidation, and then the electrolyte was taken for EEM analysis.

3. Results and discussion

3.1. Characterization of MCE anode

To identify the crystalline structure and morphology of MCE, the material was characterized by using XRD, SEM and TEM. Fig. 1a showed the mixed crystalline phases, which consisted of dominant crystal peaks accounting for Ti_4O_7, and some individual peaks indexed as crystals of Ti_5O_9 and Ti_9O_{17} (MDI Jade 5.0). All these titanium suboxides phases exhibited good conductivity (900–1050 S cm^{-1}) and similar electrochemical properties [36,37], making them suitable for electro-oxidation process. Compared with rutile TiO_2 having only edge-shared octahedron strings connected to each other via shared corners, the Ti_4O_7 has face-sharing Ti_2O_9 dimers connected with shared corner and edges every fourth octahedral, which results from the partial reduction of titanium and the migration of vacancies [38]. The reduction degree enables fine-tuning of the electrical conductivity, showing excellent metallic behavior at room temperature. The conductivity is enhanced with the degree of Ti reduction with the formula from $Ti_{10}O_{19}$ to Ti_4O_7 [36].

As illustrated in Fig. 1b, the as-prepared MCE material has a homogeneous macroscopic porous structure with the pore size ranging from 0.5 to 2 mm, and the magnified image showed an interlaced architecture of smooth blocks with pore size of 0.5–1 μm (Fig. 1c). These large pores and thick skeletons (0.8–1.5 mm) give the roughness factor of 500, accounting for electrochemically active area being 2–3 orders of magnitude higher than the apparent surface area of bulk electrode [X]. Additionally, the macroporous structure allowed uniform distribution of reactant at the thin boundary layer near the electrode, which facilitated the mass transfer within the inner pores of electrode. Besides, HRTEM characterization revealed the Ti_4O_7 (120) crystal plane with a lattice distance of 0.339 nm (insert in Fig. 1d). This crystal face should be the most obvious one compared with other crystal faces of MCE due to the highest peak intensity among the all reflective peaks as presented in XRD patterns at the 2θ angle of 26.3° (Fig. 1a). This result was similar with previously synthesized nanotube arrays of Magnéli-phase titanium suboxides [28]. Moreover, the as-prepared MCE exhibited good conductivity (0.4 Ω cm^{-1} in Fig. 1b) and mechanical strength, making it particularly suitable electrode materials for electrochemical oxidation.

A stepwise increase in potential was implemented by recording current response to show water oxidation potential in Na_2SO_4 electrolyte. There was a negligible response of current when the potential was below 2.0 V. Further increasing potential resulted in an apparent enhancement of current, indicating the potential for water oxidation should be within the potential range of 2.0–2.5 V versus SCE (Fig. 1d), indicating the capability of MCE to generate •OH radicals during water oxidation [39].

3.2. Electrochemical deactivation of M. aeruginosa

The as-prepared MCE was tested for deactivation of *M. aeruginosa* based on batch-fed electrolysis. The initial algal cell density was about 1.14–1.23 × 10^{10} cells L^{-1}, and then was recorded every 30 min during electro-oxidation with MCE anode by applying current density in the range of 1–10 mA cm^{-2}. As shown in Fig. 2a, the decrease in the cell density of *M. aeruginosa* was positively correlated with the current density and reaction time, the two essential parameters controlling the reactivity and overall efficiency. This was in accordance with prior studies where other types of algae were deactivated by electrochemical method [14,15]. The MCE proceeded with deactivation more efficiently at lower current density (1 mA cm^{-2}) than other reported anode materials (Ti–RuO_2 and BDD anodes, the current density higher than 2.5–3 mA cm^{-2}) [14,17]. For the higher current density of 2.5–10 mA cm^{-2}, the algal cell densities tended to decrease fast to 0.67–0.83 × 10^{10} cells L^{-1} after a reaction time of 60 min whereas more gently to the final value of 0.66–0.76 × 10^{10} cells L^{-1}. Higher current density increased the inhibition ratio of algae and shortened the electrolysis time. Unlike the notable difference observed in decrease of cell density for current density of 1 mA cm^{-2}, 2.5 mA cm^{-2} and 5 mA cm^{-2}, the discrimination of cell densities for 5 mA cm^{-2} and 10 mA cm^{-2} appeared less significant and the final algal cells were reduced to 0.68 × 10^{10} cells L^{-1} and 0.64 × 10^{10} cells L^{-1}, respectively. That is, the cell density varied greatly with the current density and reaction time in a specific region, which also coincided well with the results reported in prior studies [40,41].

It was noticed that the lysis of algal cells caused the decrease in apparent cell density during electrolysis. On the other hand, however, some incompletely degraded residuals and dead corpse still had contribution to the measured number of algal cells. This could explain the reason why the maximum removing efficiency was maintained a relatively low level (<52%). In order to further evaluate the algal deactivation efficiency, the chlorophyll-*a* concentration was also recorded. Cyanobacteria are known to have only one type of chlorophyll, *i. e.* chlorophyll-*a* together with blue

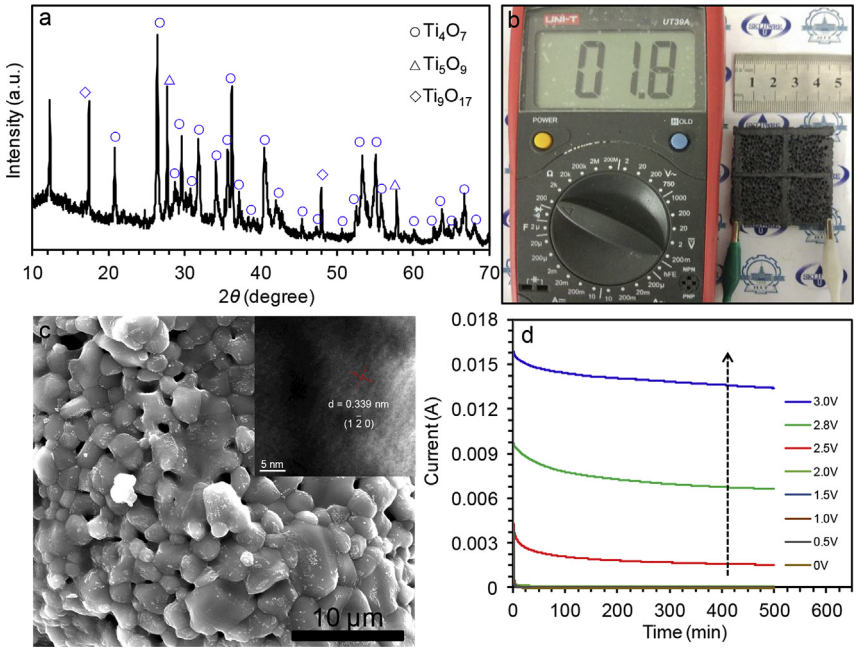

Fig. 1. (a) XRD pattern of as-prepared MCE, (b) optical, (c) SEM and HRTEM (insert) images of MCE, and (d) amperometric curves during electrolysis in 0.5 mol L^{-1} Na_2SO_4 electrolyte at various electrode potentials.

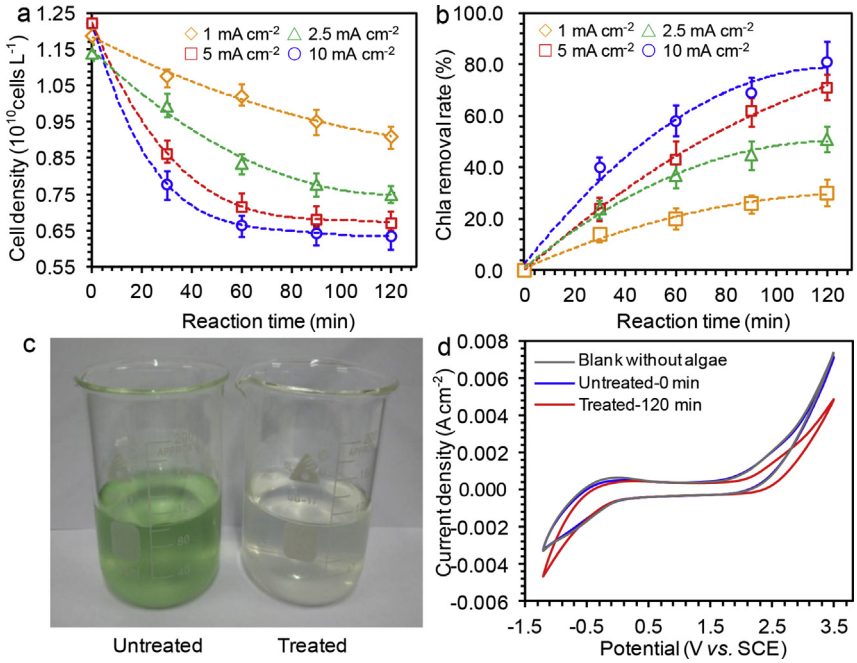

Fig. 2. Time course of (a) algal cell density and (b) Chlorophyll-*a* removal at different current densities during electrolysis, (c) the optical image of solution before and after treatment, and (d) CV scan in BG-11 medium at scan rate of 50 mV s^{-1}. The error bars ± S.D. represent the measurement in triplicate.

phycobilins, causing the blue and green color in water. Fig. 2b reveals the dependence of chlorophyll-*a* removal on current density and reaction time. Increasing the current density from 1 mA cm^{-2} to 10 mA cm^{-2} increased the chlorophyll-*a* removing efficiency from 35.1% to 89.2% after reaction time of 120 min. Unlike algal cell density, the chlorophyll-*a* removal behaved in a different manner at current density of 5 mA cm^{-2} and 10 mA cm^{-2}. That is, the variation of chlorophyll-*a* concentration appeared to be correlated insignificantly with the number of algal cells, suggesting that the electro-oxidation mainly destructed the cell integrity and components. Since the chlorophyll-*a* released from algal cells could be further degraded by electro-oxidation, the maximum chlorophyll-*a* removal rate could be obtained by 89.2%, indicating the existence of residual chlorophyll-*a* in algal cells or released into the solution. This phenomenon was also observed in prior studies where the algae was deactivated by ozone oxidation or copper sulfate [42,43].

The color of algal suspensions was clearly observed to change from green to yellow-green to light yellow and finally transparent

along with gradual degradation of chlorophyll-*a* (Fig. 2c). Fig. 2d presented the CV curves of the MCE electrode in blank (no algae), untreated and treated algal suspensions using BG-11 medium. The oxygen evolution potential in untreated algal suspensions at current density of 1.03 mA cm^{-2} was +2.37 V versus SHE, a value slightly lower than that reported in the literature [28]. After 120-min electrolysis, the surface of MCE electrode altered progressively, giving the oxygen evolution potential of +2.58 V at the same criterion. No obvious difference in the shape of CV curves was found for the blank and algal solution, indicating that the *M. aeruginosa* were mainly deactivated via indirect electrochemical oxidation mediated by oxidative species rather than direct interaction with electrode. Based on the same potential, the current density was decreased when algae were added, possibly due to the blockage of active sites by algae. To verify the decrease in current density resulting from the blockage of actives sites by algae, we performed the CV test of MCE adsorbed by *M. aeruginosa* under disconnected conditions for 120 min. The resultant CV curve almost overlapped with that for the test of "treated-120 min", indicating the adsorption of algae for decrease in current density under the same potential (data not shown).

3.3. The Re-cultivation of M. aeruginosa

Despite the maximum chlorophyll-*a* removal of 89.2% obtained, it remained unclear whether the destructed algal cells were capable of propagation and proliferation. Thus, the cell suspensions treated at different total coulombs were re-cultured for a period of 8 days at the optimum light irradiation and temperature (30 °C). As illustrated in Fig. 3, the untreated samples (*i. e.* control group), as expected, showed the fastest rate at which the algal cells could grow. When the coulombs were lower than 46.44 C, the *M. aeruginosa* were still capable of proliferation, indicated by slow increase of algal cell density within the first four days and subsequent fast growth in the subsequent four days. The re-growth rate was shown to be adversely correlated to the overall coulombs passed during electrolysis. For the total coulombs of 0–46.44 C, the peak cell density was decreased from 6.51 × 10^{10} cells L^{-1} to 3.35 × 10^{10} cells L^{-1} at the end of 8-day re-cultivation, indicating insufficient coulombs required for production of oxidative species.

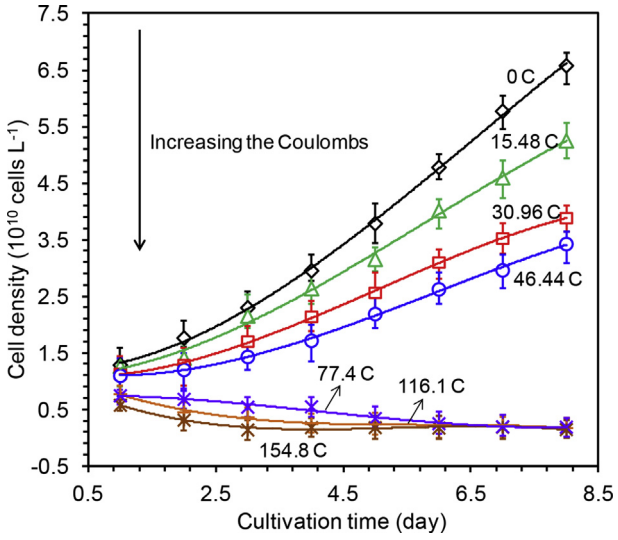

Fig. 3. Re-cultivation experiments of *M. aeruginosa* after electrolysis by MCE at different coulombs applied. The error bars ± S.D. represent the measurement in triplicate.

Applying higher coulombs (77.4–154.8 C) resulted in almost colorless solution and undetectable algal cell density when the electrolysis was stopped, suggesting the successful deactivation of *M. aeruginosa* by MCE electrode.

3.4. Electrochemical stability

The long-term stability of MCE for algal removal was investigated by conducting cyclic voltammetry experiments under a current density of 10 mA cm^{-2}. During a 50-cycle operation, the maximum chlorophyll-*a* removal (89.2%) exhibited negligible decline (Fig. 4), demonstrating a remarkable stability of MCE anode for long-term deactivating *M. aeruginosa*. The excellent stability of MCE was also verified by 5000-cycle scan without obvious loss in ORR peak current in O_2-saturated alkaline solution, and slight current loss at high potential range and high temperature after 3000-cycle CV scan in strong acidic condition [23,44]. In our previous study, the electrochemical accelerated life-span tests were performed by recording potential with respect to time under extreme and harsh conditions of 3.0 mol L^{-1} H_2SO_4 and applied current density of 1.0 A cm^{-2}. The results showed the average life time of MCE was estimated to be 30 years, a value much longer than most commonly used carbon material (7 years) [26]. According to the thermodynamics of oxygen defective Magnéli phases in rutile, the oxygen vacancies tend to be ordered in planes at low oxygen chemical potentials, forming the Magnéli phases. The spin polarization lowers the normalized defect formation energies marginally. For Ti_4O_7 and Ti_5O_9, the lowering magnitude is in the order of 0.06 eV, which has an insignificant impact on the stable ordering of these Magnéli phases. Besides, the relationship between the oxygen partial pressure and temperature at the Ti_4O_7 and Ti_5O_9 equilibrium point differs slightly, implying the insignificant impact of spin to thermodynamic stability of the crystalline structure [45]. It was worth noting that higher current density and potential may lead to the deactivation of electrode, in association with the deactivation of outside surface of Ti_4O_7 and Ti_5O_9 thin film. The performance of cleaned MCE was examined after the operation for 30 days. The deactivation efficiency could be almost completely recovered after physical cleaning by sonication for 10 min, indicating the effective removal of algae cells attached on the anode surface during long-term operation.

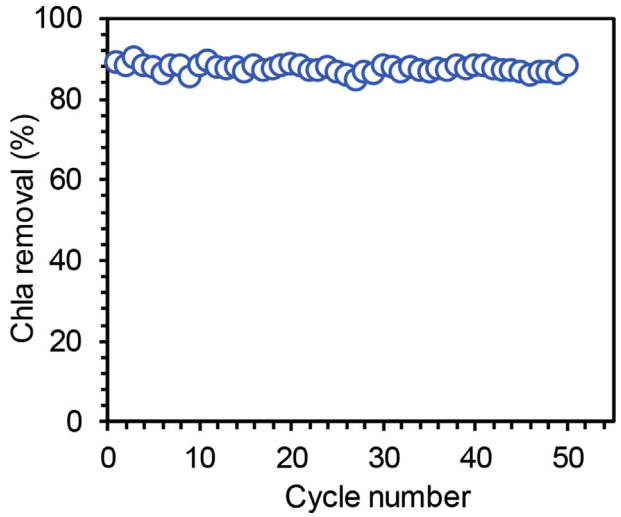

Fig. 4. The stability of MCE electrode for chlorophyll-*a* removal during 50-cycle operation.

3.5. Destruction of algal cells

In general, the electrochemical destruction of cyanobacteria can take place through direct and/or indirect mechanisms [46,47]. In the former case, the direct electron transfer takes place between electrode and cells, where the cellular component such as coenzyme A is oxidized to dimeric coenzyme A, leading to cell death by inhibiting the respiratory activity. More commonly, the indirect pathway occurs via the oxidation of algal cells by reactive oxidative species produced at relatively high potential on the anode. Bejan et al. [48] reported the ability of Ti_4O_7 to oxidize water to produce •OH and the Ti_4O_7 bounds •OH more loosely and less abundantly in physisorbed state. In addition, the active chlorine in the form of ClO^- (pK_a of 7.44) can also be produced. It is more likely for MCE to deactivate *M. aeruginosa* with electrochemically produced oxidative species of physisorbed •OH and HClO, and aqueous ClO^-. Furthermore, the released organic matters like cell cytoplasm and debris may also be oxidized to carbon dioxide and water. The •OH radicals formed during electrolysis were influenced significantly by the anode materials [49,50]. Here the unique chemical and structural properties of MCE make it a suitable anode material to form •OH radicals for algal deactivation. The production of •OH radicals on MCE was examined on the qualitative basis by using *p*-benzoquinone (*p*-BQ) as probe molecule targeting •OH radicals ($k = 1.2 \times 10^9\ M^{-1}s^{-1}$) [51]. The introduction of *p*-BQ (1 mmol L^{-1}) led to 63.2% increase in cell density and 75.5% decline in Chla removal during 120-min electrolysis, suggesting the action of •OH radicals produced from water oxidation (Fig. S1).

The AFM and SEM characterizations were used to observe the morphology of algal cells before and after electrolysis by MCE at the current density of 10 mA cm^{-2}. As shown in Fig. 5a and c, the fresh *M. aeruginosa* cells have some excreted substances on the surfaces. Compared with regular, integrated, and uniformly spherical algal cells (3–6 μm) observed for untreated samples, the 120-min electrolysis by MCE anode led to a severe collapse of cell structure, isolation of intracellular components and dissolution of cytoplasm-like substances (Fig. 5a and c).

The apoptosis and necrocytosis of *M. aeruginosa* cell could be quantitatively determined by using Flow Cytometric (FC) measurements based on Annexin V-propidium iodide (PI) double staining. Annexin V is a sensitive indicator of cells in early apoptosis by combining with cell membrane through phosphatidylserine exposed out of cells after apoptosis [52]. As nucleic acid dye, PI can make cell nucleus appear red after passing through the cell membrane. Since only the membrane of middle-to-late apoptotic and necrotic cell is selectively penetrable for PI, the viable cells, viable apoptotic cell, non-viable apoptotic cell and necrotic cells can be distinguished by the synergistic effect of Annexin V and PI [53]. As shown in Fig. 6a, the untreated samples contained 26.1% viable cells and only 0.3% necrotic cells. That is, both viable and nonviable cells existed in the control suspensions, as the tested *M. aeruginosa* cells could be harvested at initial stationary growing phase where the growth and decay rate were evenly matched in theory, causing dying of some cells naturally during cultivation process. Following 90-min electrolysis at current density of 10 mA cm^{-2}, the proportion of apoptotic and necrotic cells were found to increase considerably, reaching a remarkable level of 87.1% and 12.3% (Fig. 6b). The alive cyanobacteria can be efficiently destroyed by electro-oxidation of MCE anode. The 120-min electrolysis resulted in almost complete damage of the *M. aeruginosa* cells, indicated by the detectable viable cells of only 0.097% and nearly no survival cell (Fig. 6c). The FC results coincided well with the above results given in Figs. 2 and 3, accompanying the irreversible damage of *M. aeruginosa* cells during electrochemical oxidation induced by •OH radicals and active chlorine produced on MCE.

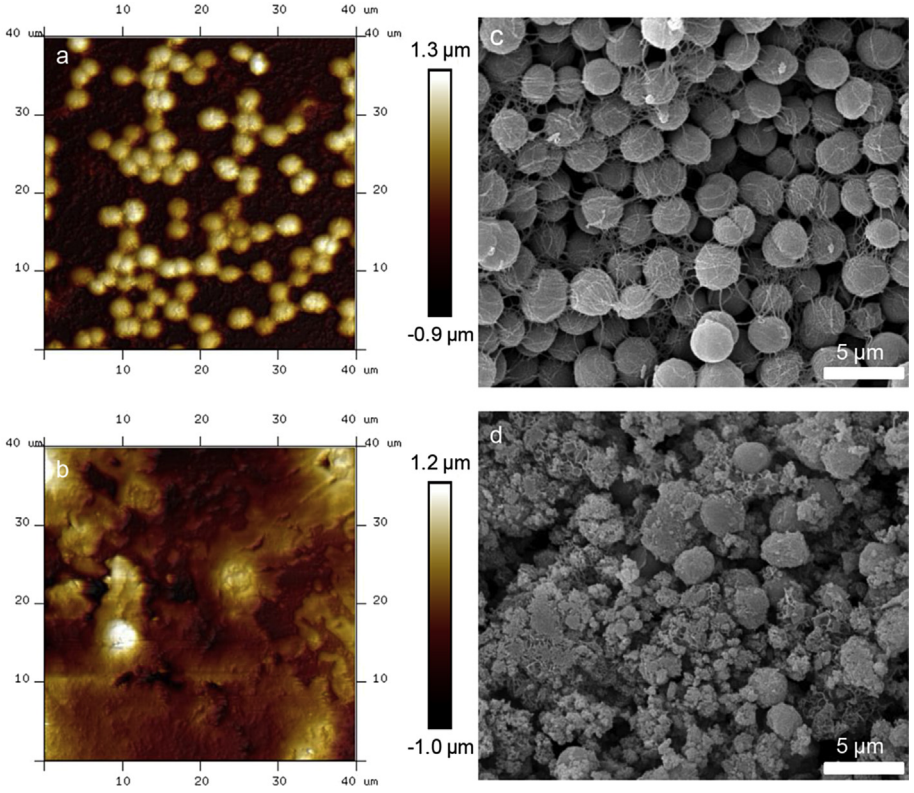

Fig. 5. AFM and SEM images of *M. aeruginosa* cells (a,c) before and (b,d) after 120-min electrolysis by MCE.

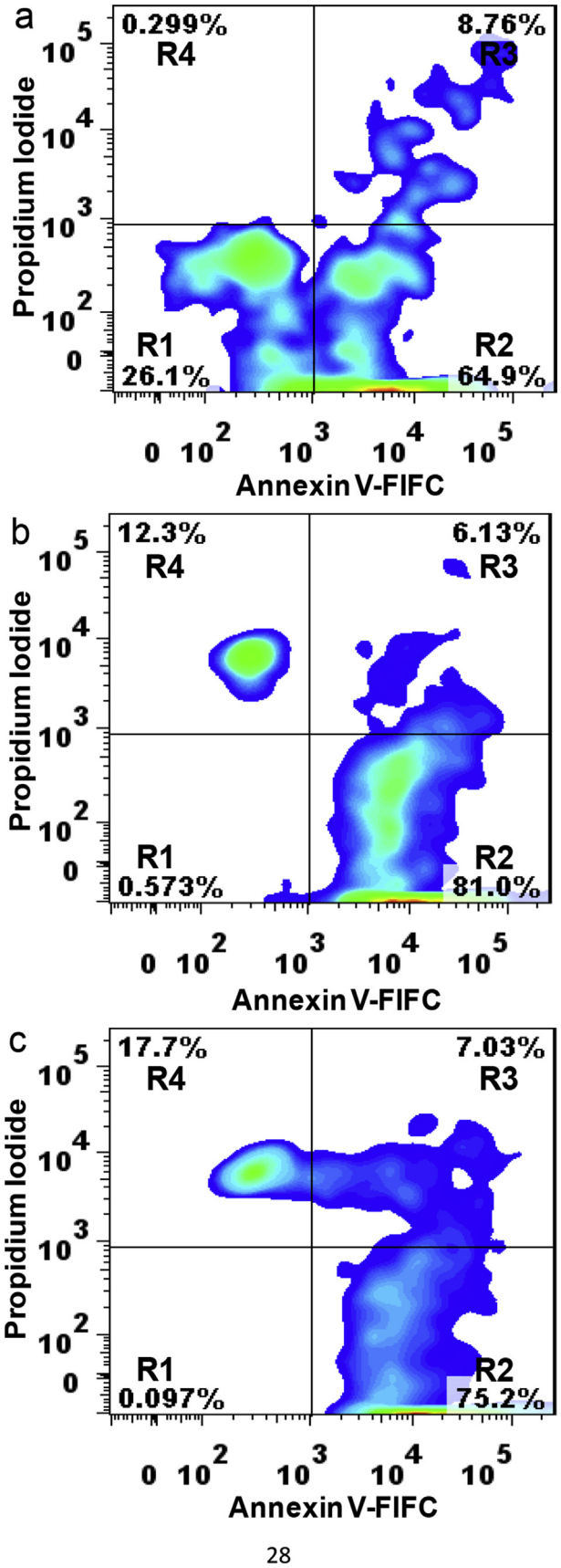

Fig. 6. The flow cytometry measurement of sample after electrolysis of (a) 0 min, (b) 90 min, and (c) 120 min by MCE. The quadrant marked with R1, R2, R3, and R4 represents the viable cells, viable apoptotic cell, non-viable apoptotic cell, and necrotic cells, respectively.

3.6. pH variation and excitation emission matrix identification

The algal solution pH was observed to increase from initial 8.0 to 9.8 at the end of 120-min electrolysis, and the increased pH value showed positive dependence on the current density applied (Fig. 7a). It is known that the anodic water oxidation releases H^+ while the cathodic water reduction produces the equivalent OH^-. Since the electrolysis was carried out under magnetic mixing condition, the combination of H^+ and OH^- could be promoted by forced convection mass transfer and thus the pH-splitting can be minimized in bulk solution. This could be verified from the inconspicuous pH fluctuation of the reacted electrolyte in the absence of *M. aeruginosa*. Since the electrochemically produced oxidative species (•OH radicals and active chlorine) is sufficiently powerful to attack and destruct the algal cells, the pH variation should be associated with the algogenic organic matters released during electro-oxidation, which were characterized by using 3D excitation-emission matrix (EEM) fluorescence spectra.

The untreated samples exhibited only one characteristic peak at excitation/emission wavelengths of 242–310 nm/270–400 nm (Fig. 7b), representing the protein-like substances contained in algal cells [54]. By the end of 30-min electrolysis, the protein-relevant peaks were shifted, and meanwhile two new additional peaks began to emerge at wavelengths of 240–280 nm and 320–380/410-500 nm, respectively (Fig. 7c). These peaks indicated the existence of humus-like substances produced from the breakage of algal cell [55]. As the electrolysis proceeded at the time of 30–120 min, the intensity and area of regions accounting for protein and humus-like substances were further decreased and increased, respectively (Fig. 7c–f). This suggests that the macromolecular cytoplasm contained in the *M. aeruginosa* cells can be oxidized and decomposed to small-molecule matters during electrolysis by MCE. The released cellular contents involve chlorophyll-*a*, microcystin, and a variety of proteins, which may be converted to ammonium through the pathway of de-aminization. At the same time, the fatty hydrocarbon and sugar-like matters could be mineralized to CO_2 and H_2O. The dissolution of ammonium and carbonates may constitute one most likely reason for pH increase observed (Fig. 7a). A number of previous studies reported that the alkaline environment is more beneficial for •OH generation in traditional electro-oxidation process [56,57], making it more effective oxidize the algal cells and further the cellular substances.

3.7. Application and implications

The feasibility of MCE anode for electrochemical deactivation of algae is demonstrated in this study. The MCE anode can achieve effective and stable removal of chlorophyll-*a* and thus *M. aeruginosa* at current density of 10 mA cm^{-2} upon the reaction time of 120 min, and the deactivated algae is shown to completely lose the ability of survival and proliferation. The results obtained

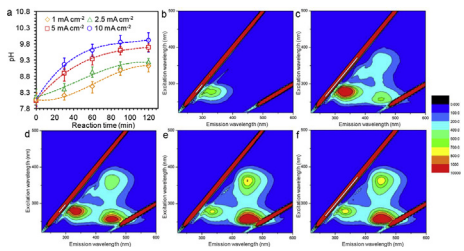

Fig. 7. (a) pH variation and 3D excitation-emission matrix (EEM) fluorescence spectra of the sample treated by electrolysis of (b) 0 min, (c) 30 min, (d) 60 min, (e) 90 min and (f) 120 min. The error bars ± S.D. represent the measurement in triplicate.

here are superior to previously reported deactivation of *M. aeruginosa* by using Ti–RuO_2 electrode [14,15]. The electrogenerated •OH radicals and active chlorine can attack the *M. aeruginosa*, leading to the bursting of cell wall and membrane, and isolation of intracellular components. Since the MCE shows similar properties with commonly used BDD, it is reasonable to prospect that MCE electrode possesses the potential ability to inactivate the *Chlorella vulgaris* algae and/or other species of harmful algae according to reported *C. volgaris* inhibition by BDD [17]. The MCE represents a promising anode material for removing algae from water in many practical applications where eutrophication may be a concern. The MCE electrode has many unique properties such as good conductivity, excellent stability, and high oxygen evolution potential. Notably, a major attraction of MCE is that it can be produced from TiO_2, a commodity chemical that is readily available and environmentally friendly across the world. All these factors would make the electrode preparation and operation process more economically reliable and more sustainable for deactivation of algae. This study provides important insights for the promising electrode material to be used for efficient and sustainable electrochemical deactivation of algae in water treatment.

4. Conclusions

Based on the above results, we demonstrated the MCE for electrochemical deactivation of *M. aeruginosa*, the most frequently detected algae in water environment. The maximum chlorophyll-a removal efficiency of 89.2% could be obtained at current density of 10 mA cm^{-2} at 120 min. The re-cultivation experiment illustrated that the coulombs in excess of 77.4 C could completely deprived the *M. aeruginosa* cells of propagation and proliferation. The deactivation of algae was associated with the oxidative species electrochemically produced on MCE. Taken together, as a new electrode material with outstanding electrical conductivity approaching to that of metals and great corrosion resistance approaching that of ceramic materials, MCE will offer a promising anode material for electrochemical deactivation of algae in potential application of water purification.

Acknowledgements

Project supported by the National Natural Science Foundation of China (No. 51678184, 51378143) and State Key Laboratory of Urban Water Resource and Environment (Grant No. 2017DX12), HIT Environment and Ecology Innovation Special Funds (No. HSCJ201610), and Natural Science Foundation of Heilongjiang Province of China (No. E2016034).

Appendix A. Supplementary data

Supplementary data related to this article can be found at https://doi.org/10.1016/j.electacta.2017.10.127.

References

[1] P. Morand, X. Briand, Excessive growth of macroalgae: a symptom of environmental disturbance, Bot. Mar. 39 (2009) 491–516.
[2] B. Petrusevski, A. Vlaski, A.N.V. Breeman, G.J. Alaerts, Influence of algal species and cultivation conditions on algal removal in direct filtration, Water Sci. Technol. 27 (1993) 211–220.
[3] A. Jelmert, J.V. Leeuwen, Harming local species or preventing the transfer of exotics? Possible negative and positive effects of using zinc anodes for corrosion protection of ballast water tanks, Water Res. 34 (2000) 1937–1940.
[4] L. Chen, J. Chen, X. Zhang, P. Xie, A review of reproductive toxicity of microcystins, J. Hazard. Mater. 301 (2016) 381–399.
[5] L. Ying, Z. Jian, B. Gao, S. Feng, Combined effects of two antibiotic contaminants on *Microcystis aeruginosa*, J. Hazard. Mater. 279 (2014) 148–155.
[6] X. Yang, W. Guo, Q. Shen, Formation of disinfection byproducts from chlor(am)ination of algal organic matter, J. Hazard. Mater. 197 (2011) 378–388.
[7] Y.L. Zhang, B.P. Han, B. Yan, Q.M. Zhou, Y. Liang, Genotoxicity of disinfection by-products (DBPs) upon chlorination of nine different freshwater algal species at variable reaction time, Aqua 63 (2014) 12.
[8] M. Baresova, M. Pivokonsky, K. Novotna, J. Naceradska, T. Branyik, An application of cellular organic matter to coagulation of cyanobacterial cells (*Merismopedia tenuissima*), Water Res. 122 (2017) 70–77.
[9] B. Ghernaout, D. Ghernaout, A. Saiba, Algae and cyanotoxins removal by coagulation/flocculation: a review, Desalin. Water Treat. 20 (2010) 133–143.
[10] M.D. Bai, Q.L. Zheng, Y.P. Tian, Z.T. Zhang, C. Chen, C. Cheng, X.Y. Meng, Inactivation of invasive marine species in the process of conveying ballast water using •OH based on a strong ionization discharge, Water Res. 96 (2016) 217–224.
[11] C.A. Martínez-Huitle, M.A. Rodrigo, I. Sirés, O. Scialdone, Single and coupled electrochemical processes and reactors for the abatement of organic water pollutants: a critical review, Chem. Rev. 115 (2015) 13362–13407.
[12] J. Radjenovic, D.L. Sedlak, Challenges and opportunities for electrochemical processes as next-generation technologies for the treatment of contaminated water, Environ. Sci. Technol. 49 (2015) 11292.
[13] M. Okochi, N. Nakamura, T. Matsunaga, Electrochemical killing of microorganisms using the oxidized form of ferrocenemonocarboxylic acid, Electrochim. Acta 44 (1999) 3795–3799.
[14] W. Liang, J. Qu, L. Chen, H. Liu, P. Lei, Inactivation of *Microcystis aeruginosa* by continuous electrochemical cycling process in tube using Ti/RuO_2 electrodes, Environ. Sci. Technol. 39 (2005) 4633.
[15] Y. Xu, J. Yang, M. Ou, Y. Wang, J. Jia, Study of *Microcystis aeruginosa* inhibition by electrochemical method, Biochem. Eng. J. 36 (2007) 215–220.
[16] M. Mascia, S. Monasterio, A. Vacca, S. Palmas, Electrochemical treatment of water containing *Microcystis aeruginosa* in a fixed bed reactor with three-dimensional conductive diamond anodes, J. Hazard. Mater. 319 (2016) 111–120.
[17] M. Mascia, A. Vacca, S. Palmas, Electrochemical treatment as a pre-oxidative step for algae removal using Chlorella vulgaris as a model organism and BDD anodes, Chem. Eng. J. 219 (2013) 512–519.
[18] Y.J. Long, H.N. Li, X. Xing, J.R. Ni, Enhanced removal of *Microcytis aeruginosa* in BDD-CF electrochemical system by simple addition of Fe^{2+}, Chem. Eng. J. 325 (2017) 360–368.
[19] X. Chen, G. Chen, F. Gao, P.L. Yue, High-performance Ti/BDD electrodes for pollutant oxidation, Environ. Sci. Technol. 37 (2015) 5021–5026.
[20] B. Xu, Y.S. Hong, Y. Mohassab, Y. Lan, Structures, preparation and applications of titanium suboxides, RSC Adv. 6 (2016) 79706–79722.
[21] J.F. Baumard, D. Panis, A.M. Anthony, A study of TiO system between Ti_3O_5 and TiO_2 at high temperature by means of electrical resistivity, J. Solid State Chem. 20 (1977) 43–51.
[22] A.A. Gusev, E.G. Avvakumov, A.Z.H. Medvedev, A.I. Masliy, Ceramic electrodes based on Magnéli phases of titanium oxides, Sci. Sinter. 39 (2007) 51–57.
[23] X. Li, A.L. Zhu, W. Qu, H. Wang, R. Hui, L. Zhang, J. Zhang, Magnéli phase Ti_4O_7 electrode for oxygen reduction reaction and its implication for zinc-air rechargeable batteries, Electrochim. Acta 55 (2010) 5891–5898.
[24] E. Slavcheva, V. Nikolova, T. Petkova, E. Lefterova, I. Dragieva, T. Vitanov, E. Budevski, Electrocatalytic activity of Pt and PtCo deposited on Ebonex by BH reduction, Electrochim. Acta 50 (2005) 5444.
[25] Y. Yang, M.R. Hoffmann, Synthesis and stabilization of blue-black TiO_2 nanotube arrays for electrochemical oxidant generation and wastewater treatment, Environ. Sci. Technol. 50 (2016) 11888–11894.
[26] S. You, B. Liu, Y. Gao, Y. Wang, C.Y. Tang, Y. Huang, N. Ren, Monolithic porous magnéli-phase Ti_4O_7 for electro-oxidation treatment of industrial wastewater, Electrochim. Acta 214 (2016) 326–335.
[27] A.M. Zaky, B.P. Chaplin, Porous substoichiometric TiO_2 anodes as reactive electrochemical membranes for water treatment, Environ. Sci. Technol. 47 (2013) 6554–6563.
[28] P. Geng, J. Su, C. Miles, C. Comninellis, G. Chen, Highly-ordered Magnéli Ti_4O_7 nanotube arrays as effective anodic material for electro-oxidation, Electrochim. Acta 153 (2015) 316–324.
[29] P. Geng, G. Chen, Magnéli Ti_4O_7 modified ceramic membrane for electrically-assisted filtration with antifouling property, J. Membr. Sci. 498 (2015) 302–314.
[30] D. Kearney, D. Bejan, N.J. Bunce, The use of Ebonex electrodes for the electrochemical removal of nitrate, Can. J. Chem. 90 (2012) 666–674.
[31] S. El-Sherif, D. Bejan, N.J. Bunce, Electrochemical oxidation of sulfide ion in synthetic sour brines using periodic polarity reversal at Ebonex® electrodes, Can. J. Chem. 88 (2010) 928–936.
[32] O. Scialdone, A. Galia, G. Filardo, Electrochemical incineration of 1,2-dichloroethane: effect of the electrode material, Electrochim. Acta 53 (2008) 7220–7225.
[33] Z. Ertekin, U. Tamer, K. Pekmez, Cathodic electrochemical deposition of Magnéli phases Ti_nO_{2n-1} thin films at different temperatures in acetonitrile solution, Electrochim. Acta 163 (2015) 77–81.
[34] M. Ma, S.J. You, G.S. Liu, J.H. Qu, N.Q. Ren, Macroporous monolithic Magnéli-phase titanium suboxides as anode material for effective bioelectricity generation in microbial fuel cells, J. Mater. Chem. A 4 (2016) 18002–18007.
[35] D. Burrini, E. Lupi, C. Klotzner, C. Santini, E. Lanciotti, Survey for microalgae and cyanobacteria in a drinking-water utility supplying the city of Florence, Italy, J. Water Supply Res. Technol.-AQUA 49 (2000) 139–147.

[36] S. Harada, K. Tanaka, H. Inui, Thermoelectric properties and crystallographic shear structures in titanium oxides of the Magnèli phases, J. Appl. Phys. 108 (2010) 083703–083706.
[37] C. Tang, D. Zhou, Q. Zhang, Synthesis and characterization of Magnéli phases: reduction of TiO_2 in a decomposed NH_3 atmosphere, Mater. Lett. 79 (2012) 42–44.
[38] X. Tao, J. Wang, Z. Ying, Q. Cai, G. Zheng, Y. Gan, H. Huang, Y. Xia, C. Liang, W. Zhang, Strong sulfur binding with conducting Magnéli-phase $Ti_{(n)}O_{2(n-1)}$ nanomaterials for improving lithium-sulfur batteries, Nano Lett. 14 (2014) 5288–5294.
[39] M.H.P. Santana, L.A.D. Faria, J.F.C. Boodts, Electrochemical characterisation and oxygen evolution at a heavily boron doped diamond electrode, Electrochim. Acta 50 (2005) 2017–2027.
[40] G. Chen, Electrochemical technologies in wastewater treatment, Sep. Purif. Technol. 38 (2004) 11–41.
[41] M. Panizza, C. Bocca, G. Cerisola, Electrochemical treatment of wastewater containing polyaromatic organic pollutants, Water Res. 34 (2000) 2601–2605.
[42] F. Benoufella, A. Laplanche, V. Boisdon, M.M. Bourbigot, Elimination of microcystis cyanobacteria (blue-green algae) by an ozoflotation process: a pilot plant study, Water Sci. Technol. 30 (1994) 245–257.
[43] C.W.K. Chow, M. Drikas, J. House, M.D. Burch, R.M.A. Velzeboer, The impact of conventional water treatment processes on cells of the cyanobacterium *Microcystis aeruginosa*, Water Res. 33 (1999) 3253–3262.
[44] C. Yao, F. Li, X. Li, D. Xia, Fiber-like nanostructured Ti_4O_7 used as durable fuel cell catalyst support in oxygen reduction catalysis, J. Mater. Chem. 22 (2012) 16560–16565.
[45] L.R. Liborio, Thermodynamics of oxygen defective Magnéli phases in rutile: a first-principles study, Phys. Rev. B 77 (2008) 104104.
[46] T. Matsunaga, S. Nakasono, T. Takamuku, J.G. Burgess, N. Nakamura, K. Sode, Disinfection of drinking water by using a novel electrochemical reactor employing carbon-cloth electrodes, Appl. Environ. Microbiol. 58 (1992) 686–689.
[47] L.V. Venczel, M. Arrowood, M. Hurd, M.D. Sobsey, Inactivation of cryptosporidium parvum oocysts and clostridium perfringens spores by a mixed-oxidant disinfectant and by free chlorine, Appl. Environ. Microbiol. 63 (1997) 4625.
[48] D. Bejan, E. Guinea, N.J. Bunce, On the nature of the hydroxyl radicals produced at boron-doped diamond and Ebonex® anodes, Electrochim. Acta 69 (2012) 275–281.
[49] L. Szpyrkowicz, S.N. Kaul, N.N. Rao, S. Satyanarayan, Influence of anode material on electrochemical oxidation for the treatment of tannery wastewater, Water Res. 39 (2005) 1601–1613.
[50] D.M. Jacobowitz, A.T. Kallarakal, Influence of anode material on the electrochemical oxidation of 2-naphthol: Part 2. Bulk electrolysis experiments, Electrochim. Acta 48 (2003) 3491–3497.
[51] M. Rueffer, D. Bejan, N.J. Bunce, Graphite: an active or an inactive anode? Electrochim. Acta 56 (2011) 2246–2253.
[52] C. Smith, D.F. Gibson, F.J. Tait, Transmembrane voltage regulates binding of annexin V and lactadherin to cells with exposed phosphatidylserine, BMC Biochem. 10 (2009) 1–8.
[53] R.I. Daly, L. Ho, J.D. Brookes, Effect of chlorination on *Microcystis aeruginosa* cell integrity and subsequent microcystin release and degradation, Environ. Sci. Technol. 41 (2007) 4447–4453.
[54] F. Qu, H. Liang, Z. Wang, H. Wang, H. Yu, G. Li, Ultrafiltration membrane fouling by extracellular organic matters (EOM) of *Microcystis aeruginosa* in stationary phase: influences of interfacial characteristics of foulants and fouling mechanisms, Water Res. 46 (2012) 1490.
[55] W. Chen, P. Westerhoff, J.A. Leenheer, K. Booksh, Fluorescence excitation-emission matrix regional integration to quantify spectra for dissolved organic matter, Environ. Sci. Technol. 37 (2003) 5701.
[56] E. Brillas, C.A. Martínez-Huitle, Decontamination of wastewaters containing synthetic organic dyes by electrochemical methods. An updated. review, Appl. Catal. B Environ 166–167 (2015) 603–643.
[57] J.M. Aquino, R.C. Rocha-Filho, M.A. Rodrigo, C. Sáez, P. Cañizares, Electrochemical degradation of the reactive red 141 dye using a boron-doped diamond anode, Water Air Soil Poll. 224 (2013) 1397.